Determining representative mechanical parameters of clay matrix in mudstones using nanoindentation mapping and machine learning data analysis: a novel top seal characterization approach

Xiangyun Shi[1], David Misch[1], Stanislav Zak[2], Megan Cordill[2], Daniel Kiener[3]

[1] Department of Applied Geosciences and Geophysics, Chair of Petroleum Geology, Montanuniversität Leoben, Peter-Tunner-Straße 5, 8700 Leoben, Austria

[2] Erich Schmid Institute of Materials Science, Austrian Academy of Sciences, Jahnstraße 12, 8700 Leoben, Austria

[3] Department Materials Science, Chair of Materials Physics, Montanuniversität Leoben, Jahnstraße 12, 8700 Leoben, Austria

1. Introduction

Mudstones and shales are important top seals for various geoenergy applications, and the mechanical properties of their clay matrix play a crucial role for understanding seal capacity and failure risk. However, characterizing the mechanical properties of clay matrix at small scales is challenging. In this study, a workflow was developed using high-speed nanoindentation mapping combined with machine learning data analysis to determine representative mechanical parameters of clay matrix. The approach was tested on a mudstone top seal sample from a Vienna Basin oil field (Misch et al., 2021), and its reliability was investigated using different experimental settings. This study represents an important methodological step towards the high-throughput micromechanical characterization of mudrocks.

2. Methods

Nanoindentation mapping

The sample (~1629 m; quartz 31 wt.%, clay mineral 39 wt.%) was polished using a Hitachi ArBlade 5000 broad ion beam (BIB) system and imaged using a Tescan Clara field emission scanning electron microscope (SEM) before and after the nanoindentation. Nanoindentation property mapping was performed using a Hysitron TS 77 Select Nanoindenter in load-controlled mode (see also Vranjes-Wessely et al., 2021). A total of eight array maps (7 × 7 indents, 6 µm spacing) were indented, covering both grain and matrix areas (Fig. 1). Maps 1-5 tested the effect of different indenter tips (Maps 1-2 with the Berkovich tip and Maps 3-5 with the Cube Corner tip) and the sensitivity of the indentation depth with an increasing maximum load from 500 to 1500 µN. Maps 6-8 tested the load rate sensitivity using the Cube Corner tip at a single maximum load of 1000 µN and decreasing loading rates of 6000, 3333, and 1000 µN s^{-1}. The obtained load-displacement curves were used to determine E_r and H after the Oliver-Pharr method (Oliver and Pharr, 1992).

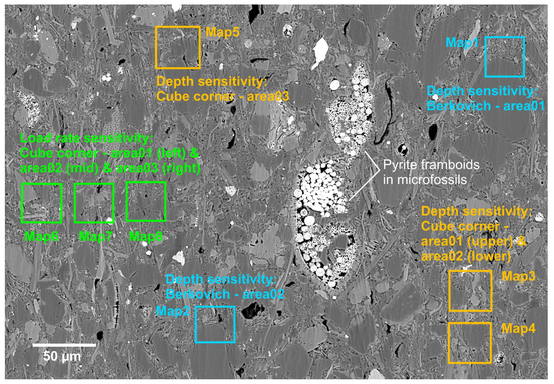

Fig. 1. Position of the indentation maps with different experimental setups. The distinctive structure of the pyrite cement in microfossils helped in locating targeted testing area during nanoindentation.

k-means clustering

The *k*-means algorithm in the Python library scikit-learn (Pedregosa et al., 2011) was utilized to classify different phases and determine representative mechanical properties of the clay matrix. Before clustering, the load-displacement curves were quality-checked to filter out artefacts or invalid results. *k*-means clustering analysis was performed using three input features including hardness (H), reduced elastic modulus (E_r), and the elastic-plastic deformation ratio based on the obtained load-displacement curves. The number of clusters was set to three to capture the three main classes including clay matrix, others, and grain. To validate the *k*-means clustering results, the residual indentation impression and the constituent materials under the residual imprint were identified in the SEM images.

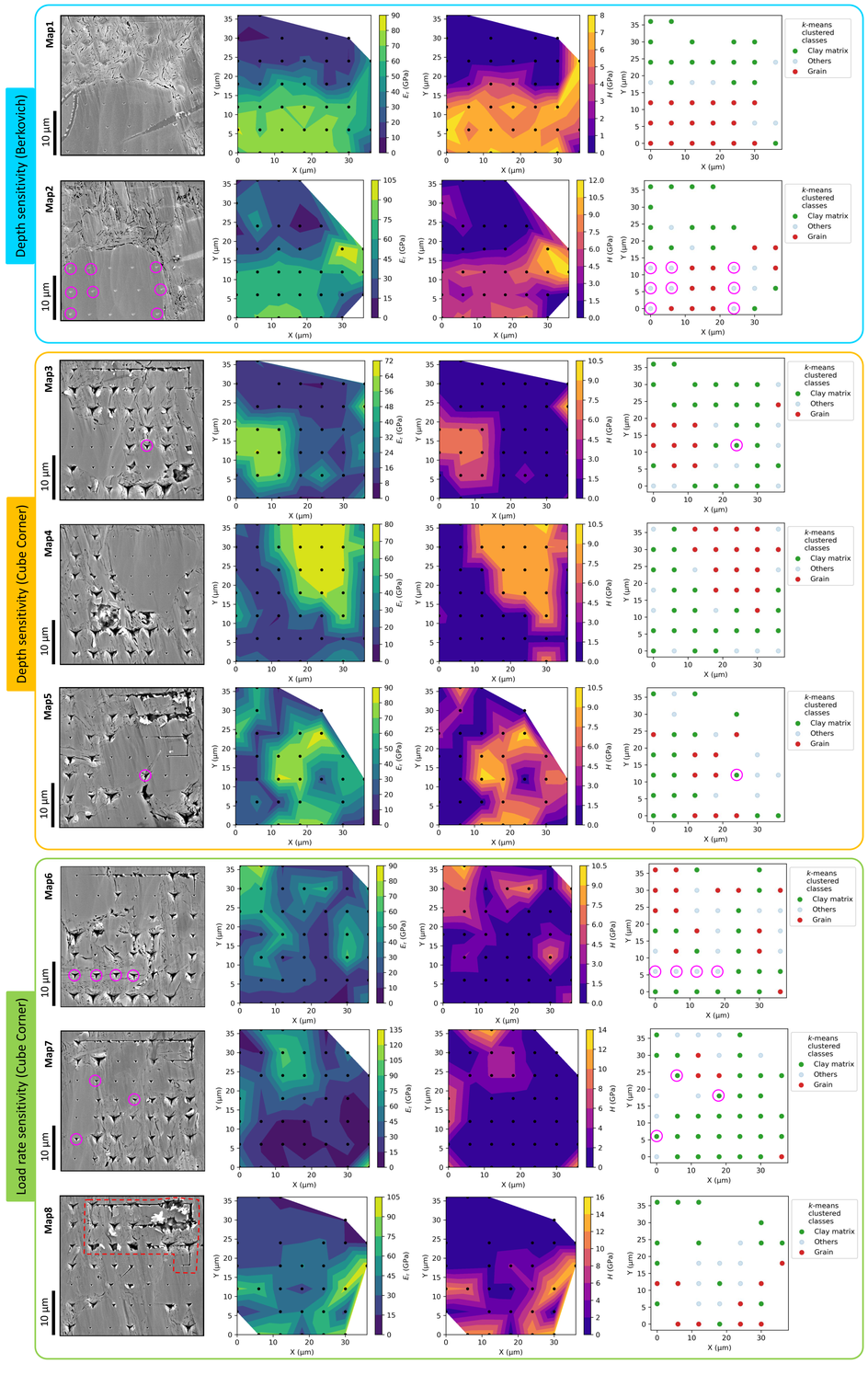

Fig. 2. SEM images, correlative E_r and H property maps, and the *k*-means clustering results of Maps 1-8. SEM images reveal visible indentation imprints after indentation mapping. Linear interpolated E_r and H property maps are based on valid indents. The *k*-means clustering of the valid indents are colour coded. The magenta circles highlight possibly debatable classification. The red dashed line encloses an area of strong surface damage.

3. Results

The *k*-means clustering efficiently classified three distinct classes and showed an overall good correlation with the SEM images (Fig. 2). The classification of some indents located at grain boundaries (classified as “others”) may be subject to debate or uncertainty (highlighted magenta circles in Fig. 2). The residual impressions on the maps produced by the Cube Corner tip are visually much deeper compared to those by the Berkovich tip. The property maps reveal distinct regions of the indented grain and clay matrix areas. Decreasing the load rate from 6000 to 1000 µN s^{-1} resulted in unstable indentation testing and stronger surface damage, suggesting the sensitivity of the clay matrix to the loading rate.

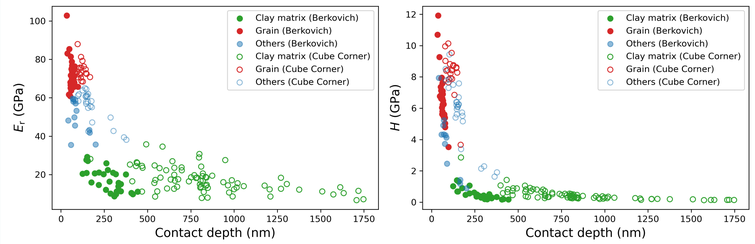

Fig. 3. E_r- and H- contact depth profiles for Maps 1-5. The colour code of data points corresponds to the *k*-means clustering results in Fig 2.

Fig. 3 shows the obtained E_r and H values plotted against indentation contact depth for Maps 1-5, with the Cube Corner tip sampling deeper depths compared to the Berkovich tip. The highest indentation depths for the clay matrix indented by the Cube Corner tip are much deeper than those indented by the Berkovich tip (~150 to 440 nm for the Berkovich tip vs. ~500 to 1750 nm for the Cube Corner tip). Despite this, the E_r and H values for the “clay matrix” class obtained by both tips are in a similar range, with average E_r and H values of 16.23 ± 6.16 GPa and 0.5 ± 0.49 GPa (n=151), respectively. The “grain” and “others” classes show sharp decrease in E_r and H values over a relatively small depth range, while the “clay matrix” class shows slight fluctuations but remains generally constant. This suggests that the mechanical properties of the clay matrix are not as sensitive to the indentation depth as other phases. Testing with both tips shows that representative values can be determined from minimum volumes with statistical significance, despite the strongly heterogeneous microstructure of the indented clay matrix.

4. Conclusions and Outlook

This contribution represents an important methodological step towards the implementation of combined high-speed nanoindentation mapping and machine learning data analysis as a feasible high throughput tool for the micromechanical characterization of mudstones and similar fine-grained sedimentary rocks. The presented approach is planned to be applied to an extensive set of mudstone samples from the Vienna Basin with the purpose to link mechanical property changes to burial diagenesis.

Acknowledgments

The authors thank OMV for providing the mudstone samples and permission to publish the data from the Vienna Basin. Lukas Skerbisch and Gerhard Hawranek are thanked for their help with image acquisition. This study was funded by the Austrian science fund FWF (grant no. P 33883).

Contact: Xiangyun.shi@unileoben.ac.at

References

Misch, D., Siedl, W., Drews, M., Liu, B., Klaver, J., Pupp, M., Sachsenhofer, R.F., 2021. Mineralogical, Bib-Sem and Petrophysical Data in Seal Rock Analysis: A Case Study from imaging and machine learning data analysis. International Journal of Coal Geology 247, 103847. https://doi.org/10.1016/j.coal.2021.1the Vienna Basin, Austria. Journal of Petroleum Geology 44, 25–46. https://doi.org/10.1111/jpg.12777

Oliver, W.C., Pharr, G.M., 1992. An improved technique for determining hardness and elastic modulus using load and displacement sensing indentation experiments. Journal of materials research 7, 1564–1583.

Pedregosa, F., Varoquaux, G., Gramfort, A., Michel, V., Thirion, B., Grisel, O., Blondel, M., Prettenhofer, P., Weiss, R., Dubourg, V., 2011. Scikit-learn: Machine learning in Python. the Journal of machine Learning research 12, 2825–2830.

Vranjes-Wessely, S., Misch, D., Kiener, D., Cordill, M.J., Frese, N., Beyer, A., Horsfield, B., Wang, C., Sachsenhofer, R.F., 2021. High-speed nanoindentation mapping of organic matter-rich rocks: A critical evaluation by correlative imaging and machine learning data analysis. International Journal of Coal Geology 247, 103847. https://doi.org/10.1016/j.coal.2021.103847